# Breaking of Key Layers and Surface Subsidence in the Loess Mountainous Areas



# Breaking of Key Layers and Surface Subsidence in the Loess Mountainous Areas

**Ke Lv and Jinan Wang**

School of Civil and Resource Engineering, University of Science and Technology Beijing, Beijing, China

**Abstract.** During the process of mining subsidence, the thick loess layer will have certain cohesion, tensile strength and flexural strength. Therefore, the thick loess layer may have a significant impact on the overburden load of the mining area, which further affects the fracture and surface subsidence of the overlying strata on the working surface. The calculation model was constructed based on the mining geological conditions of the loess mountainous area in Jinhe Coal Mine of Gansu Province. The mining surface and process were simulated by FLAC$^{3D}$, and the load effect of loess layer thickness on its lower strata and its key layers was analyzed. The results show that the surface loess layer is mainly caused by tensile failure, and the other rock layers are mostly shear failure. The key layer has obvious control effect on surface settlement, and its fracture can lead to significant settlement on the surface. Under the condition of thick loess layer, the initial breaking distance of the key layer is larger than that of the critical mining length. The results show that the equivalent load coefficient of the loess layer is obtained and applied to the calculation of the fracture distance, which can obtain more realistic parameters.

**Keywords:** loess layer; surface rock movement; key layer; subsidence

## 1. Introduction

The western China is rich in coal resources, and most of the coal mines are located in mountainous areas with complex topography. Along with a large amount of coal resources, surface subsidence and environmental disasters caused by underground mining have become increasingly prominent, and seriously affect the ecological environment of the mining area and the safety of surface buildings [1]. In order to guide the deployment of mining face and protect the ground buildings, it is necessary to study the characteristics of stratum fracture and surface movement deformation for underground mining in mountain areas. Affected by mountainous terrain, the conventional mining subsidence prediction theory is not applicable in mountainous terrain. The expected results are often quite different from the measured results [2], lacking scientific and reliable rock movement data [3-4].

At the same time, the thickness of the loess layer in the western coal mine is generally large, and the topography and geomorphology of the loess mountainous area is complex, which itself belongs to the multi-region of geological disaster area [5]. In the area of mining subsidence, the mining subsidence in the Loess Mountain area is expected to be more complicated [6]. In the mining area with thin topsoil, the key layer plays a major role in controlling the surface subsidence [7]. Under the condition of thick loess cover, the mining subsidence can be regarded as the result of the joint action of underground excavation and loess layer [8]. Because loess is a special stratum with appropriate adhesion and shear strength, the mining subsidence law under its influence is also unique [9-10].

At the beginning of the last century, the formation of mining subsidence disciplines has formed representative classical theories such as masonry beam hypothesis [11], key layer theory [12] and pallet theory [13], which greatly enriched the study of mining subsidence. direction. On this basis, a series of new methods for studying mining subsidence were proposed. At present, there are methods such as probability integration method [14], theoretical model method [15], numerical calculation method [16-18], similar material simulation method [19] and artificial neural network prediction method [20]. In recent years, numerical calculation has been widely used. Li Fei et al. [21] verified the existence of overburden cantilever beam structure during high-slope mining and low-slope mining from numerical analysis and actual observation, and explained the local uplift of the slope bottom. phenomenon. Liu Wensheng et al. [22] used probability integral method and FLAC$^{3D}$ to study the discontinuous failure of overburden igneous rocks in goaf, and considered that igneous rocks are protective and abrupt to their upper strata. These theoretical and numerical methods are useful for studying the influence of thick loess layer on settlement.

Based on the background of Jinhe Coal Mine, the FLAC$^{3D}$ numerical simulation software is used to simulate the movement and failure of overlying strata under the influence of thick loess layer. The loading effect of loess layer thickness on its lower strata, especially the key layer, is analyzed. Combined with the results of on-site rock movement monitoring, some understandings on the theory of overburden damage in the loess mountainous area are proposed.

## 2. Project Overview

No.1 well of Jinhe Coal Mine is located at the junction of Gansu and Qinghai provinces, the northern part of the loess sag of the Loess Plateau in the Loess Plateau, and the “Hebei Valley” in the northwestern part of the desert steppe ash-calcium land. The terrain in the minefield is complex, and the gully is developed, almost all of which is covered by the loess layer, forming landforms such as ping, raft, beam and raft. These loess girders with varying degrees of erosion and severe erosion, and the inter-mountain basins filled with recent floods and the narrow valleys of multi-level terraces represent the geomorphic features of the Yaojie area. The mine field has the characteristics of high mountain height, deep valley, many soils and few stones. The terrain is high in the north and low in the south. The altitude is between 2100 and 2450 m, and the relative height is 100-350 m. It has the shape of the Loess Plateau in central Guizhou. Loess in the mine field, color brown yellow, gray yellow, loose, large porosity, strong capillary action, easy to see through water, water leakage.

The main coal-bearing section of the Jinhe coalfield consists of coal seams, black carbonaceous mudstones, medium-fine sandstones, and siltstones. The lower part is black carbonaceous mudstone, medium-fine sandstone, pebbled fine sandstone sandwiched coal seam, the middle part is extra-thick and thick coal seam (coal two-layer); the upper part is siltstone, carbonaceous mudstone and thin oil shale interbed, top There is a layer of high gray peat (one layer of coal). The 16201, 16203, 16205, and 16207 working faces are located between 605m and 620m with an average thickness of 10m. Figure 1 is a schematic view of a mining area, and Figure 2 is a typical sectional view of a mining area with a profile of P1-P1 in Figure 1.

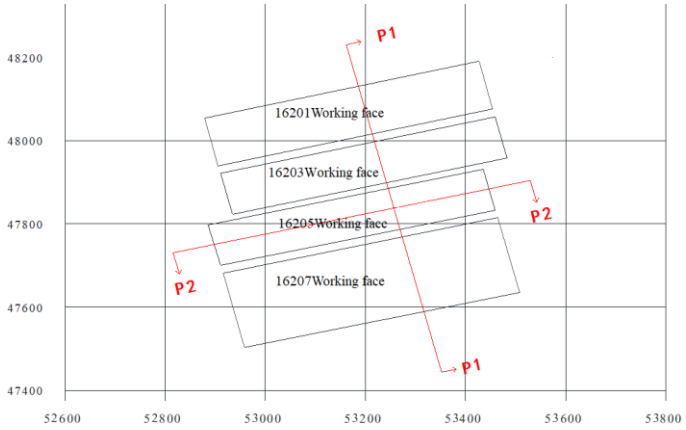


**Figure 1.** Schematic diagram of the mining area

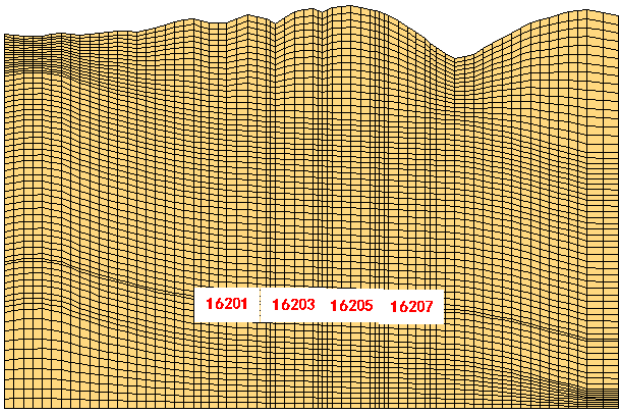


**Figure 2.** Section P1-P1 of mining area

### 3. Establishment of Flac Numerical Model

This study uses FLAC$^{3D}$ to calculate and analyze the mechanical process of fully mechanized mining in 3D stope. In order to comprehensively and systematically reflect the stress and deformation of the surrounding rock in Jinhe Coal Mine during the development process and operation state, this study is based on the Jinhe Coal Mine Engineering Geological Report, Jinhe Coal Mine Mining Project Plan and related materials. A three-dimensional computing model based on the FLAC$^{3D}$ program.

In order to fully reflect the mechanical behavior of the rock mass in the mining area as much as possible, the numerical calculation model area covers almost the entire area of the Jinhe coal mine, including all mining work since the self-built mine. According to the engineering geological data, the model rock formation is initially simplified into four layers, from the top to the bottom, the Quaternary system, the Jurassic system on the Jurassic system, the Jurassic Zhongjie Yaojie group, and the Jurassic system. In order to accurately analyze the vicinity of the coal seam, the Jurassic system and the Jurassic Zhongjie Yaojie Group were subdivided. The Jurassic system is divided into three layers, and the Jurassic Zhongtong Yaojie Group is divided into seven layers. The total stratum of the model is fourteen. Figure 3 is a schematic diagram of a three-dimensional model grid. The calculation model is 1300m long and 1300m wide. The bottom of the model is about 908m high from the bottom to the surface. There are 314160 grid cells and 328233 nodes.

Static boundary conditions are applied during the initial equilibrium phase: the four sides of the

model are rolling bearings that limit horizontal movement and the bottom of the model limits vertical movement. In the calculation of dynamics, the bottom of the model is a viscous boundary and the periphery is a free-domain boundary. In order to more reasonably reflect the effect of real tectonic stress, the measured geostress is simulated as the original rock stress field of the model according to the linear difference method.

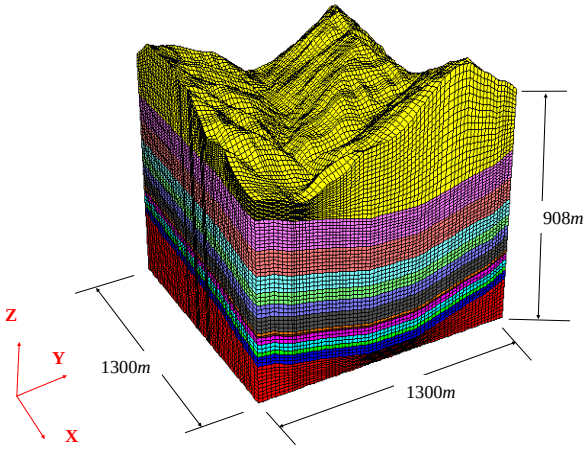


**Figure 3.** 3D numerical model grid diagram of Jinhe Coal Mine

According to the results of rock mechanics tests provided by on-site geological survey and related research, considering the alteration of the rock part, the mechanical properties of the core and the altered part are tested respectively. Among them, the altered part of the rock dominates the overall properties of the rock. effect. According to the actual situation of the site and the relevant geological data, the final numerical parameters are shown in Table 1.

**Table 1.** Rock layer mechanical parameters

| Lithology | Thickness | Density | Modulus of elasticity | Poisson's ratio | Internal friction angle | Cohesion | Tensile strength | Shear modulus | Bulk modulus |
|---|---|---|---|---|---|---|---|---|---|
| | m | $kg/m^3$ | MPa | | ° | MPa | MPa | MPa | MPa |
| Loess layer | 165 | 1800 | 500 | 0.3 | 21 | 1.8 | 0.36 | 192.31 | 416.67 |
| Sandstone | 100 | 2450 | 3500 | 0.24 | 35 | 2.1 | 1.18 | 1411.3 | 2243.6 |
| Siltstone-1 | 86 | 2700 | 3410 | 0.2 | 35 | 2 | 1.29 | 1420.8 | 1894.4 |
| Mudstone-1 | 58 | 2180 | 1500 | 0.22 | 34 | 1.9 | 0.73 | 614.8 | 892.9 |
| Fine Sandstone | 42 | 2720 | 3150 | 0.11 | 35 | 2.35 | 1.2 | 1418.9 | 1346.2 |
| Mudstone-2 | 43 | 2180 | 1500 | 0.22 | 34 | 1.9 | 0.73 | 614.8 | 892.9 |
| Siltstone-2 | 54 | 2700 | 3410 | 0.2 | 35 | 2 | 1.29 | 1420.8 | 1894.4 |
| Mudstone-3 | 10 | 2180 | 1500 | 0.22 | 34 | 1.9 | 0.73 | 614.8 | 892.9 |
| Coal-1 | 6 | 1370 | 627.5 | 0.25 | 20.74 | 0.9 | 0.61 | 251.0 | 418.3 |
| Coarse Sandstone-1 | 25 | 1370 | 627.5 | 0.25 | 20.74 | 0.9 | 0.61 | 251.0 | 418.3 |
| Coal-2 | 27 | 1370 | 627.5 | 0.25 | 20.74 | 0.9 | 0.61 | 251.0 | 418.3 |
| Siltstone-3 | 15 | 2778 | 3627.5 | 0.23 | 35 | 2 | 1.29 | 1474.6 | 2239.2 |
| Coarse sandstone-2 | 34 | 2720 | 3200 | 0.23 | 40 | 2.6 | 1.35 | 1300.8 | 1975.3 |
| Siltstone-4 | 250 | 2778 | 3627.5 | 0.23 | 35 | 2 | 1.29 | 1474.6 | 2239.2 |

The entire simulation process is as follows: First, simulate the state before unexcavation. By establishing the original stratigraphic model, applying the displacement constraint boundary conditions, iterative calculation is performed under the initial stress conditions to achieve the stress balance of the system. Then, according to the actual mining sequence in the field, the working face is recovered, and the historical variables to be tracked are set in time. Set the support structure and iterate to make the model reach equilibrium and stable state. The mining sequence and mining technical parameters of the working face are shown in Table 2.

**Table 2.** Working face mining sequence and mining technical parameters

| Mining No. | Working face name | Thickness | Depth | Stride length | Prone width |
|---|---|---|---|---|---|
| | | m | m | m | m |
| 1 | 16201 | 10.21 | 610 | 565 | 120 |
| 2 | 16203 | 10.25 | 620 | 565 | 100 |
| 3 | 16205 | 10.11 | 605 | 565 | 100 |
| 4 | 16207 | 10.01 | 615 | 565 | 180 |

## 4. Simulation and Measurement Results of Mining Subsidence

### *4.1. Surrounding Rock Failure and Settlement in Inclined Direction*

The development of the surrounding rock failure field on the P1-P1 section after mining in the mining face is shown in Figure 4. After the working face is excavated, the surrounding rock damage is concentrated on the top and bottom plates, and the depth of the roof plate is slightly larger than the height at which the floor plate is damaged. With the successive excavation of the subsequent working faces, the damage of the overburden increases due to the disturbance of the adjacent working faces, and the damage of the bottom plate remains basically stable. When the mining of 16201 working face is completed, a small amount of continuous plastic failure zone is formed along the periphery of the goaf. The main damage is mainly shear failure. The damage range extends from 610m from the ground to 460m from the ground. 4(a). In the mining stage of 16203 working face, as the working face increases, more continuous plastic failure zones are formed along the periphery of the goaf. The main damage is mainly shear failure, as shown in Figure 4(b). At this stage, the plastic damage range extends up to 356 m from the ground.

The mine has entered the large working face mining since the 16205 working face, that is, the working face length is increased and the mining speed is increased. As shown in Figure 4(c), the failure field is mainly concentrated around the goaf and above the roof, and the main failure mode is still shear failure. A plastic failure zone occurred in the stratum at 274 m from the ground, and the damage still did not reach the surface. After the end of the 16207 working face, the tensile damage occurred on the surface of the top loess layer. Other areas except this are mostly shear failure, and the damage area is obviously increased, and the position is moved up as a whole. As shown in Figure 4 (d).

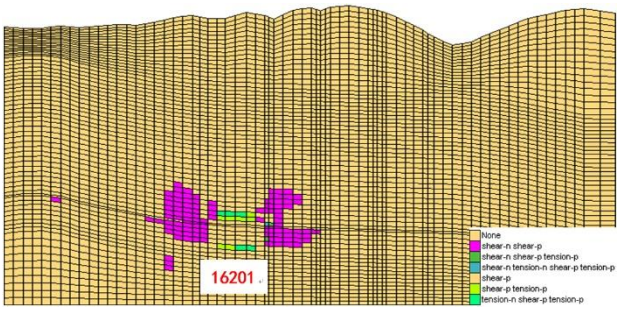

(a)16201 After mining

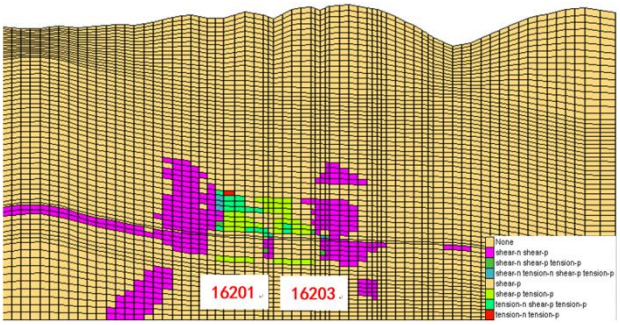


(b)16203 After mining

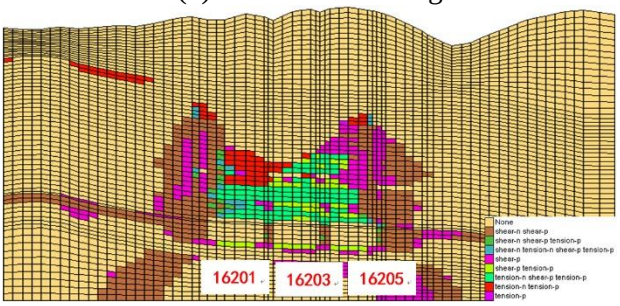


(c)16205 After mining

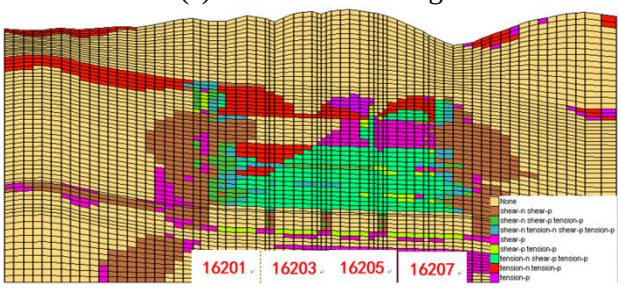


(d)16207 After mining

**Figure 4.** P1-P1 section along the coal seam tends to surrounding rock failure field

The change of the displacement field after each working face is recovered according to the above mining sequence. Figure 5 is a schematic diagram of the vertical displacement field of the P1-P1 profile. After the 16201 working face is recovered, the upper part of the goaf falls, and the falling arch is formed in the upper 5m area of the goaf. The displacement inside the arch is large, and the surrounding rock above the falling arch is relatively stable. After the mining of the adjacent 16203 working face is completed, the two goafs run through the arch and extend upwards to communicate with the overburden. As shown in Figure 5 (b).

When the 16205 working face is finished, a falling arch area is also formed in the upper part of the goaf. Although the maximum displacement point of the section is still in the early goaf, it can be seen from Figure 5(c) that above the goaf, the displacement of the upper part of the rock caving arch has gradually connected with the surface displacement, surface loess A certain degree of vertical settling also occurs in the layer. After the mining of the 16207 working face, as the area of the goaf is further increased, as shown in Figure 5(d), the settlement of the overlying rock mass is intensified. The settlement of the goaf becomes the occurrence of the maximum displacement of the section, and the overlying old rock mass has the tendency of the displacement of the same rock mass. The increase of the rock mass movement will have a greater impact on the underground mining.

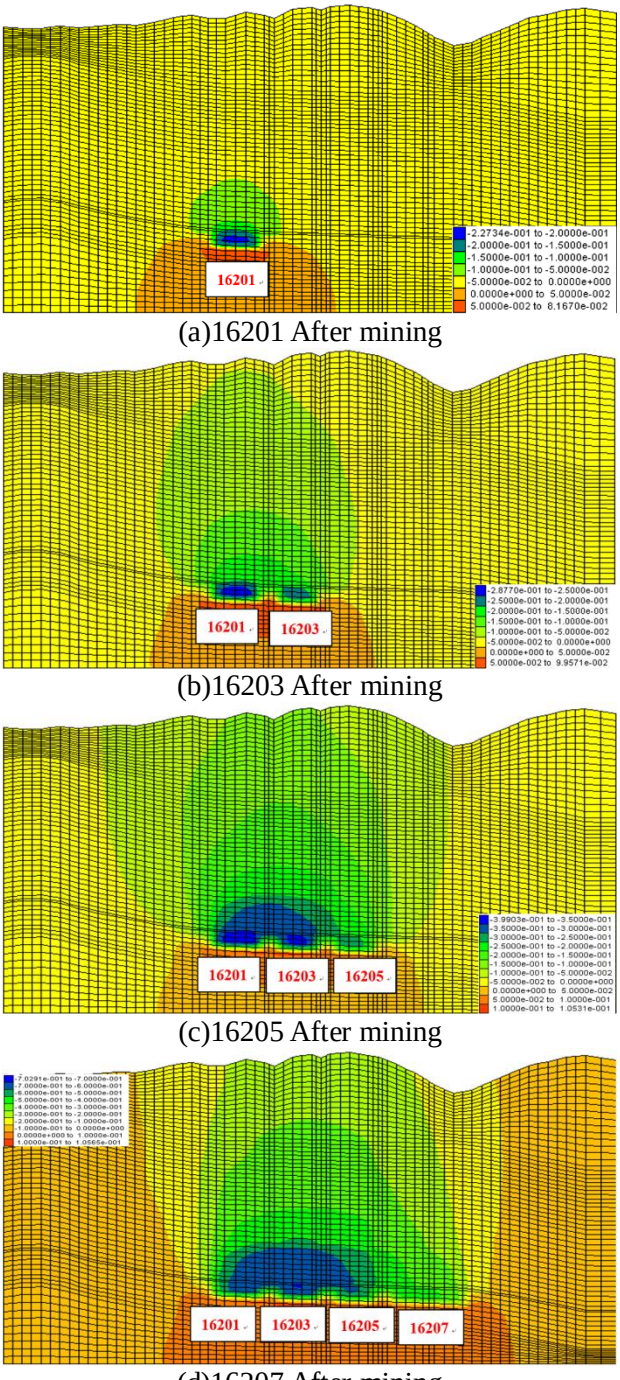


(a)16201 After mining

(b)16203 After mining

(c)16205 After mining

(d)16207 After mining

**Figure 5.** P1-P1 section along the coal seam tends to surrounding rock vertical displacement field

In summary, from the perspective of the tendency, the mining of the working face leads to the continuous extension of the overburden strata. The development range of the plastic zone shows the fracture zone of the rock formation, and the corresponding vertical displacement reflects the control range of the fractured rock formation. It can be seen that the rock formation in the range of about 200-300 m from the ground has obvious control effect on the surface settlement. The mining of the 16201 and 16203 working faces (total width of about 225m) did not break, so the vertical displacement did not reach the surface before the 16205 face was recovered. Subsequent mining of the

two working faces caused the width of the mining to be further increased, causing the rock formation to gradually break and cause the ground to settle.

*4.2. Survey of Surface Settlement on the Strike*

Due to the large difference in mining time of multiple working faces in Jinhe Coal Mine, the most complete 16205 working face mining stage with the most complete measuring point and the most complete monitoring process is analyzed.

The recovery period for the 16205 work surface is from November 7, 2013 to July 22, 2014. The segmentation progress is shown in Figure 6.

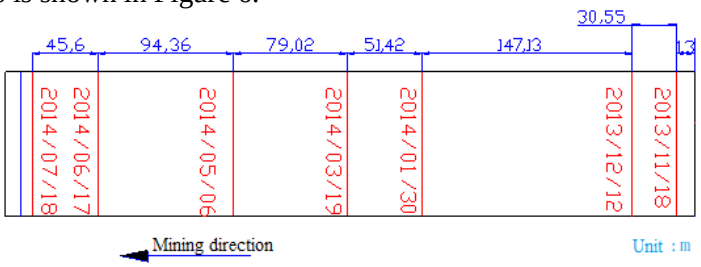


**Figure 6.** 16205 working face mining progress chart

Figure 7 shows the surface subsidence along the strike of the 16205 working face in different periods during the mining process measured by the station.

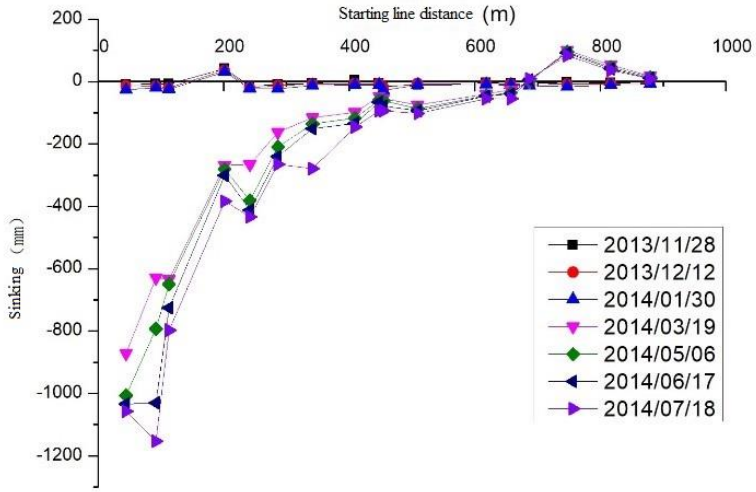


**Figure 7.** Surface settlement of 16205 working face

As shown in the above figure, at the beginning of the working face mining (November 2013 to January 2014), the surface settlement along the working face is not obvious, and the amount of change per record is not large. When the mining is completed until March 19, 2014, when the total length of mining is 230.35m, the surface subsidence phenomenon appears obviously, and the sinking curve at this time is observed and recorded. After the recovery process of 218.98m, the surface settlement continued to develop, and the settlement near the goaf was more obvious, but the settlement growth rate and the settlement curve shape did not change significantly. It can be considered that when the length of mining is 230.35m, the fracture of the rock layer that controls the surface causes the ground settlement to occur sharply.

## 5. Calculation and Optimization of Key Layers and their Breaking Distance

The settlement of the mining site is affected by many factors. Among them, the periodic fracture of the overburden caused by the mining face directly affects the degree of surface settlement. The surface subsidence curve will also be accompanied by a stepwise change of "stable-mutation-stable" with the recovery process. According to the key layer theory of rock formation control, the overlying strata in the stope are mainly controlled by a number of key layers with relatively thick thickness and hardness. Therefore, the location of the key layer is inferred according to reasonable parameters, and the initial fracture and periodic fracture distance are determined accurately. It is of great significance for the prediction and analysis of surface settlement.

### *5.1. Key Layer Calculation*

The theoretical derivation and calculation methods of the key layers have been discussed in detail in the literature [7], and will not be repeated here. Using this method, according to the stratum parameters of Jinhe Coal Mine shown in Table 1, it is judged that the key layer in the overlying strata of the stope is glutenite, and according to

$$L_c = h\sqrt{\frac{2\sigma_t}{q}} \tag{1}$$

$$L_z = h\sqrt{\frac{\sigma_t}{3q}} \tag{2}$$

The initial fracture and periodic fracture distance are calculated respectively, where $h$ is the thickness of the key layer, $\sigma_t$ is the tensile strength of the formation, and $q$ is the self-weight load of all the controlled rock layers acting on the key layer. List the key layers and their parameters as follows.

**Table 3.** Overlying load and fracture distance of key layers

| Lithology | Depth | Thickness | Overlying load | Initial breaking distance | Period breaking distance |
|---|---|---|---|---|---|
| | m | m | MPa | m | m |
| Sandstone | 165 | 100 | 2.97 | 89.14 | 36.39 |

From the theory and the above observations, it is known that the fault energy of the key layer drives the overlying strata and the loess layer to move together and directly affect the surface subsidence. Therefore, the length of the goaf and the state of the key layer can be represented as shown in Figure 8.

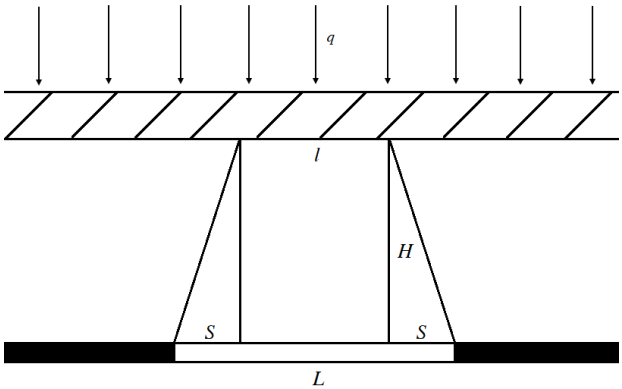


**Figure 8.** Key layer cantilever beam and gob length

In the figure, $q$ is the load on the key layer, $L$ is the length of the goaf, $S$ is the key offset of the key layer, $h$ is the thickness of the key layer, and $l$ is the length of the cantilever beam of the key layer.

It can be known from equation (2) that when satisfied

$$l < L_c \tag{3}$$

The deformation of the key layer belongs to the bending and sinking; when the length $L$ of the goaf increases to a certain size, the key layer will produce fracture and settlement under the overlying load, and the loess layer will produce significant deformation, resulting in sudden surface subsidence. Increase. The length of the goaf at this time is called the critical mining length $L_0$, then

$$L_0 = L_c + 2S \tag{4}$$

Among them, $S$ embodies the deviation of the fault zone developed above the stope, which is related to the height of the key stratum and the characteristics of the strata, i.e.

$$S = f \cdot H \tag{5}$$

Where $H$ is the height of the key layer and $f$ is the characteristic parameter of the rock layer under the key layer. Depending on the strength of the rock formation, it can be calculated from the same or similar working conditions. Available from (1)(4)(5)

$$L_0 = h\sqrt{\frac{2\sigma_t}{q}} + 2f \cdot H \tag{6}$$

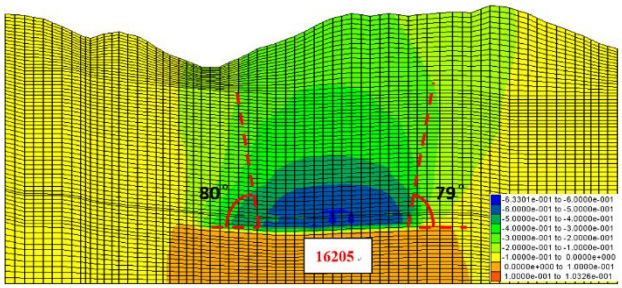


**Figure 9.** P2-P2 section along the 16205 working face to the vertical displacement field of surrounding rock

According to the numerical simulation results (Figure 9), the impact angle of the working face on the key layer, combined with the geological data provided by the site, comprehensively judge the rock layer characteristic parameters here to take $f$=0.18. The height and breaking distance of the key layer in Table 3 are brought into (6), and the critical mining length $L_0$=213.34m.

Comparing the above results with the simulated and measured results of mining subsidence, it can be found that the critical mining width in the numerical simulation results is greater than 225m; the critical layer breaking distance reflected by the sudden change of surface sedimentation curve is 230.35m, which is also larger than the calculation result. It is therefore necessary to optimize the parameters in this calculation to obtain a more accurate critical mining length.

### *5.2. Equivalent Load Benchmark Experiment of Loess Layer*

The existing literature generally applies the loess layer to the bedrock layer according to its own weight static load. This simplification basically meets the requirements for the loose sand layer or the soft clay layer. However, for structural loess with cohesive, tensile and flexural strength, part of the pressure generated by its own weight will be transferred to the rock masses on both sides, which may result in the actual pressure on the bedrock surface. Covering the loess layer has a low self-weight.

According to the literature [23], the reduction effect of this load has a certain relationship with the thickness of the loess layer and the mechanical parameters, mining width, width to depth ratio. However, some of the factors, such as the aspect ratio of the aspect ratio in this model, are close to 1, which is basically negligible. Therefore, this study focuses on the effect of the thickness of the loess layer on its load.

The FLAC$^{3D}$ software is also used to establish the benchmark model. The stratum parameters are selected in Table 1. In the calculation, the length of the mining is 500m, the mining width is 120m, and other conditions remain unchanged, only the thickness of the loess layer is changed. By replacing the loess layer and its own weight by direct load, the key layer also reaches the same maximum settlement. The definition $Q$ is the equivalent load of the loess layer acting on the key layer at this time. The equivalent load reduction factor $k$ is the ratio of the equivalent load to the self-heavy load of the loess layer. The results are listed below.

**Table 4.** Overlying load and fracture distance of key layers

| Loess layer thickness | Loess layer weight load | Loess layer equivalent load | Equivalent load reduction factor |
|---|---|---|---|
| $h_t$/m | MPa | Q/MPa | k |
| 20 | 0.36 | 0.318 | 0.882 |
| 40 | 0.72 | 0.609 | 0.846 |
| 60 | 1.08 | 0.880 | 0.815 |
| 80 | 1.44 | 1.100 | 0.764 |
| 100 | 1.8 | 1.382 | 0.768 |
| 120 | 2.16 | 1.626 | 0.753 |
| 140 | 2.52 | 1.885 | 0.748 |
| 160 | 2.88 | 2.137 | 0.742 |
| 180 | 3.24 | 2.417 | 0.746 |
| 200 | 3.6 | 2.650 | 0.736 |
| 220 | 3.96 | 2.922 | 0.738 |
| 240 | 4.32 | 3.175 | 0.735 |

According to the above results, the relationship between k and loess layer thickness $h_t$ is plotted, as shown in Figure 10.

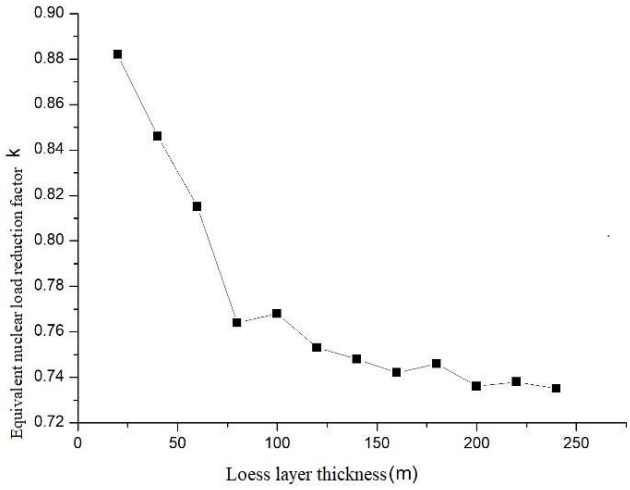


**Figure 10.** Equivalent load reduction factor and loess layer thickness curve

Its characteristics are as follows:

(1) Under the condition that the mining width and other parameters are kept unchanged, the higher the thickness of the loess layer, the greater the self-weight load, and the equivalent load that produces the same settlement effect also increases.

(2) The equivalent load reduction factor $k$ is between 0.74 and 0.89 and is negatively correlated with the thickness $h_t$ of the loess layer. The smaller the $h_t$ is, the weaker the equivalent effect of the equivalent load on the loess layer. When $h_t$ is increased to 100m, the reduction factor will continue to decrease, but tends to be stable.

### *5.3. Critical Layer Load Correction*

The load parameters in the calculation of the key layer are corrected by the experimental results of the equivalent load of the loess layer. According to the actual thickness of the loess layer of 165 m, the equivalent load reduction factor $k$=0.74. The product of the loess layer's self-weight load and k is the loess layer load, and the key layer and its parameters are recalculated. After calculation, the key layer is still determined as a glutenite layer, but its overlying load and fracture distance will change, which are listed below.

**Table 5.** Overlying load and fracture distance of the modified key layer

| Lithology | Depth | Thickness | Overlying load | Initial breaking distance | Period breaking distance |
|---|---|---|---|---|---|
| | m | m | MPa | m | m |
| Sandstone | 165 | 100 | 2.20 | 103.57 | 42.28 |

The height and breaking distance of the key layer in Table 5 are brought into (6), and the corrected critical mining distance $L_0$ =227.77m. Obviously, the revised critical mining distance is more consistent with numerical simulation experiments and field measurements.

## 6. Surface Subsidence under the Influence of Thick Loess

In this section, based on the field observation data before and after mining of 16205 working face, the surface settlement of No.1 well of Jinhe Coal Mine under the influence of thick loess layer is summarized from various aspects such as sinking, horizontal movement and deformation.

(1) sinking

In the direction of the direction, as the mining progresses, the amount of surface subsidence increases continuously, and the position of the maximum sinking point moves continuously with the working surface. At the end of mining, the surface subsidence tends to be stable. The final surface sinking amount is 1184mm.

In the direction of inclination, the earth's surface tends to sink, but the movement is relatively flat. The closer to the working surface, the greater the surface subsidence. During the process of propelling the working face, the sinking distance away from the goaf is small and gradually stabilizes; the subsidence from the goaf is large, but it eventually stabilizes.

(2) Horizontal movement

In the direction of the strike, the horizontal displacement reciprocates between positive and negative, and the surface soil moves in the mining direction. With the advancement of the mining and moving away from the working surface, the horizontal displacement gradually decreases. The maximum horizontal movement appears at a near point according to the working surface, and the value is 370.549 mm.

In the direction of inclination, at the initial stage of mining, the horizontal displacement is not large, and the horizontal displacement varies between -600mm and 100mm.

(3) Horizontal deformation

The maximum horizontal compression deformation on the strike is -35.66 mm/m, and the horizontal tensile deformation reaches a maximum of 34.99 mm/m in the same period of time. The rest

of the time has changed but does not exceed these two maximums, and the overall change is in the form of a sine wave. The horizontal deformation value tends to be in the range of -6.2 mm/m to 5.83 mm/m. The relative deformation is relatively small, and the horizontal deformation of the surface is basically stable.

(4) Tilt deformation

In general, the slope deformation gradually weakens as the mining progress progresses. Upward, the deformation fluctuates greatly within 200m from the origin. In the tendency, the range of variation in the negative direction relative to the positive direction is wide, and the maximum value increases first and then decreases. The maximum tilt deformation occurs in the goaf.

(5) Surface rock movement parameters

| Rock movement parameter | Go | Tendency |
|---|---|---|
| Maximum sinking | 1184mm | 1153mm |
| Maximum horizontal displacement | 114.667mm -802mm | -627.127mm 97.79mm |
| Maximum horizontal deformation | -37.153 mm/m 12.617 mm/m | -6.2mm/m 5.83 mm/m |
| Maximum tilt deformation | -21.127 mm/m 6.066 mm/m | -2.78 mm/m 17.23 mm/m |
| Mountain moving angle | $64.68^o$ | |
| Downhill moving angle | $62.5^o$ | |
| Surface sinking angle | $83^o$ | |
| Moving towards the corner | $55.2^o$ | |
| Sinking coefficient | 0.04 | |

## 7. Conclusion

(1) The plastic zone caused by mining activities will continue to expand as the length of the mining is increased. When the damage extends to the surface, the loess layer is dominated by tensile failure, and other areas are mostly shear failure.

(2) The rock formation in the No. 1 mine of Jinhe Coal Mine is about 200-300 m away from the ground and has obvious control effect on surface subsidence. When the length of the mining is 230.35m, the fracture of the key rock layer causes the surface settlement phenomenon to be significant.

(3) For the area where the surface is thick loess layer, if the load of the loess layer is completely simplified to its own weight load, the calculated critical layer breaking distance and critical mining length are often small.

(4) The self-weight load of the loess layer can be converted into an equivalent load to optimize the calculation of the key layer and the breaking distance. The higher the thickness of the loess layer, the greater the equivalent load.

(5) The equivalent load reduction factor is negatively correlated with the thickness of the loess layer. The smaller the thickness, the weaker the equivalent effect of the equivalent load on the loess layer. When the thickness of the loess layer is more than 100 m, the reduction effect will tend to be stable.

## References

[1] Tang Jun, Wang Jin-an, Wang Lei. Dynamic laws and characteristics of surface movement induced by mining under thin alluvium [J]. Rock and Soil Mechanics, 2014, 35(10):2958-2968+3006.

[2] Kang Jianrong. Analysis of effect of fissures caused by underground Mining on ground movement and deformation [J]. Chinese Journal of Rock Mechanics and Engineering, 2008(01):59-64.

[3] Liu Teng, Wang Jin-an, Gao Zhi-guo, Wang Li. Similarity Simulation Research of Slope Deformation During Underground Mining in Mountainous Area [J]. Metal Mine,2014(10):161-165.
[4] He Wanlong. Mining subsidence and mining damage in mountainous areas [M]. Beijing: China Science and Technology Press, 2003.
[5] Guo Xun, Dai Junwu. Analysis of building damage caused by interaction between faults and coal mining subsidence [J]. Liaoning University of Engineering and Technology (Natural Science Edition), 2006,25(6): 851-854.
[6] Mei Songhua, Sheng Qian, Li Wenxiu. New progress in mining subsidence research [J]. Chinese Journal of Rock Mechanics and Engineering, 2004, 23(1): 4535 -4538.
[7] Qian Minggao, Qi Xiexing, Xu Jialin, et al. Key layer theory of rock formation control [M]. Xuzhou: China University of Mining and Technology Press, 2003: 31-40.
[8] Tang Fuquan. Mining subsidence prediction model in western thick loess layer mining area [J]. Journal of China Coal Society, 2011, 36(S1): 74-78.
[9] Guo Wenbing, Deng Kazhong, Zou Youfeng. Research on surface movement parameters of strip-partial mining [J]. Journal of China Coal Society,2005(02):182-186.
[10] Liu Zherong, Yan Ling, He Xiao, Bao Liying, Liu Guanzhi. Effects of mining subsidence on physical and chemical properties of soil in the subsided land of the Daliuta Mining Area[J]. Journal of Arid Land Resources and Environment, 2014,28 (11): 133-138.
[11] Qian Minggao, Shi Pingwu, Xu Jialin. Mine pressure and rock formation control [M]. Xuzhou: China University of Mining and Technology Press, 2010.
[12] Mu Xiexing, Chen Ronghua, Pu Hai, et al. Analysis of breakage and collapse of Thick key strata around coal face [J]. Chinese Journal of Rock Mechanics and Engineering, 2005, 24(8): 1289-1295.
[13] Wu Lixin, Wang Jinzhuang, Liu Yan'an, et al. Theory and practice of mining coal strips under construction (structure) [M]. Xuzhou: China University of Mining and Technology Press, 1994.
[14] Liu Baozhen, Liao Guohua. Basic Laws of Surface Movement in Coal Mines [M]. Beijing: China Industrial Press, 1965.
[15] Litwiniszyn J Statistical methods in the mechanics of granular bodies [J]. Rheologica Acta, 1958, 1(2): 146-150.
[16] Li Yunpeng, Wang Zhiyin. Three-dimensional damage finite element analysis of mining settlement [J]. Rock and Soil Mechanics,2003,24(2):183-187.
[17] Guo Chunying, Li Yunlong, Liu Junzhu. UDEC in the steep thick seam mining subsidence in the application of numerical simulation [J]. China Mining Magazine,2010, 19(4):71-74.
[18] Wang Jin-an, Jiao Shen-hua, Hou Zhi-ying. Study on the catastrophic collapse of surface land induced by mining under a shallow and hard stratum [J]. Journal of China Coal 45Society,2007,32(10):1051-1056.
[19] Wang Lei, Zhang Xian-ni, Guo Guang-li, et al. Research on surface subsidence prediction model of coal mining with solid compacted backfilling [J]. Rock and Soil Mechanics,2014,35(7):1973-1978.
[20] Cao Liwen, Jiang Zhenquan. Research on Application of Artificial Neural Network in Predicting Mining Subsidence [J]. Journal of China University of Mining & Technology, 2002,31(1):23-26.
[21] Li Fei, Wang Jin-an, Li Peng-fei, Huang Kun. Research on movement behavior and failure mechanism of overlying strata caused by mining at mountainous field [J]. Rock and Soil Mechanics,2016,37(04):1089-1095.
[22] Liu Wensheng, Wu Zuoqi, Kong Jing, Cui Tiejun. Numerical simulation for the mechanism and causes of the surface cracks due to the coal seam mining [J]. Journal of Safety and Environment,2016,16(05):135-139.
[23] Tang Fuquan, Xia Yucheng, Yao Youqiang. Mining subsidence and ground protection in loess-covered mining area [M]. Beijing: Science Press, 2011.